A High Optical Transmittance and Low Cost Touch Screen without Patterning

Karim SAMADZAMINI[1], Javad FROUNCHI[1], Hadi VELADI[2]
[1]*Microelectronic and Microsensor Research Laboratory, Faculty of Electrical and Computer Engineering, University of Tabriz, Tabriz, Iran*
[2]*MEMS Research Laboratory, Faculty of Electrical and Computer Engineering, University of Tabriz, Tabriz, Iran*
corresponding.kszamini@tabrizu.ac.ir

***Abstract*—Transparent Conducting Oxide (TCO) materials such as Fluorine Tin Oxide (FTO) and Indium Tin Oxide (ITO) due to their optical and electrical properties are used in touch screens as electrodes and wires. This paper proposes a novel technique of using Electrical Resistivity Tomography (ERT) method in order to produce touch screens without pattering. Unlike existing techniques, the proposed methodology employs a uniform TCO coated screen with a maximum optical transmittance to convert the touch point coordinates into side electrodes voltages. The performance of the proposed method is tested experimentally on a FTO coated glass with a sheet resistance of 20 ohms/sq. The proposed methodology is found to be less complicated and low cost, since no pattern or electrodes are implemented in the display area.**

***Index Terms*—electric potential, electrodes, indium tin oxide, tomography, wiring.**

I. Introduction

A touchscreen is an electronic visual display that can detect the presence and location of a touch within the display area. The term generally refers to touching the display of the device with a finger or hand. Touch screens can also sense other passive objects, such as a stylus. In other words, a touch screen is any monitor, based either on LCD (Liquid Crystal Display) or CRT (Cathode Ray Tube) technology that accepts direct onscreen input. The ability for direct onscreen input is facilitated by an external (light pen) or an internal device (touch overlay and controller) that relays the X, Y coordinates to the computer [1].

Touchscreen interactive devices have become increasingly important in both consumer and commercial applications. All touchscreen technologies in use today are projected capacitive, analog resistive, surface capacitive, surface acoustic wave, infrared, camera-based optical, liquid crystal display in-cell, bending wave, force sensing, planar scatter detection, vision-based, electromagnetic resonance, and combinations of technologies[2-3]. The information provided on each touchscreen technology includes a little history, some basic theory of operation, the most common applications, the key advantages and disadvantages, a few current issues or trends, and the author's opinion of the future outlook for the technology. Touchscreen technology has the potential to replace most functions of the mouse and keyboard. The touchscreen interface is being used in a wide variety of applications to improve human computer interactions [4-5].

Transparent conducting oxide (TCO) semiconductors are widely used as transparent films in electronic devices such as thin film solar cells, displays devices, electro-chromic displays, defogging aircraft and automobile windows, gas sensors and other areas [6]. Currently, Sn doped In2O3 (ITO) is the most extensively used for such applications due to its excellent properties such as low resistivity (~ 10-4 Ω cm) and high optical transmittance (80-90%T) [7-8]. However, the abundant use of ITO as TCO thin films has several drawbacks such as scarcity, high toxicity, and expensive source of indium itself [9-10]. Numerous efforts to develop alternative materials are in progress. Fluorine doped tin oxide (FTO) is a possible alternative to ITO because FTO is inexpensive as well as chemically and thermally stable [11].

FTO exhibits good visible transparency (up 91%T), while retaining a low electrical resistivity due to the high carrier concentration [12]. FTO is mechanically and electrochemically stable, and it is utilized in numerous technologies including thin film solar cells, dielectric layers in low emissivity coatings for windows, gas sensors applications and liquid crystal displays [9], [13]. There are a number of methods/techniques to grow SnO2 (either doped or un-doped) films, including chemical vapor deposition, pulsed laser deposition, DC reactive sputtering and spray pyrolysis [14-15].

FTO coated glass is electrically conductive and ideal for use in touch screen displays, thin film photovoltaic and other electro-optical applications [16]. Fig. 1 shows TCO implementation in patterning on touch screens.

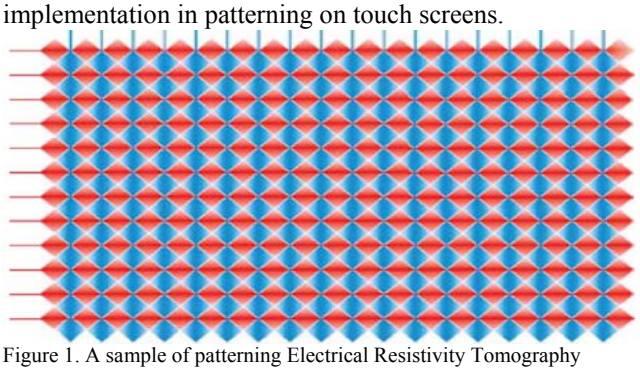

Figure 1. A sample of patterning Electrical Resistivity Tomography

A. Basis

ERT has numerous applications including geophysical, chemical engineering, medical and oil exploration, etc. [17]. In this method, the distribution of electrical resistance within the surface is achieved through measuring the electrode

Digital Object Identifier 10.4316/AECE.2017.01016

voltage beside the surface (Fig. 2). It is done by placing electrodes on the surface of a matrix, around, injecting current to them and receiving the corresponding voltage from other electrodes [18].

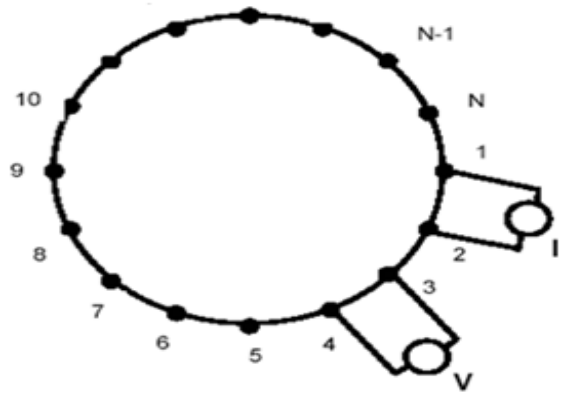

Figure 2. Sample electrode ordering in ERT

B. Fundamental Relation of Electrical Resistance Tomography

The basic physical law used in ERT is taking the form of Ohm's law for electric current density. The equation in the form of a continuous volume is as follows [19-20]:

$$\vec{J} = \sigma(x,y,z)\vec{E} \quad (1)$$

where σ is the bulk conductivity and E is the electric field. In practice, ρ(x,y,z) might be used instead of σ(x,y,z) conductivity.

However, our measurements are based on obtaining the voltage level of the surface. The relationship between electric potential(V) and electric field strength is demonstrated by the following equation:

$$\vec{E} = -\nabla\vec{V} \quad (2)$$

The combination of equations (1) and (2) yields the following equation:

$$\vec{J} = -\sigma(x,y,z)\nabla\vec{V} \quad (3)$$

Applying the principle of conservation of charge over a volume, and using the equation of continuity, we obtain:

$$\nabla.J = Q \quad (4)$$

Now, if the current on the surface is on the x_s, y_s, z_s point, the law of current continuity is obtained by the following equation:

$$\nabla.J = I\delta(x-x_s)\delta(y-y_s)\delta(z-z_s) \quad (5)$$

Where δ is the Dirac delta function.

With the combining (4) and (5) yields the elliptic Poisson's equation:

$$-\nabla\cdot(\sigma\nabla V) = Q \quad (6)$$

Therefore, this equation (3) can be rewritten as:

$$\nabla\cdot[-\sigma(x,y,z)\nabla V(x,y,z)] = I\,\delta(x-x_s)\delta(y-y_s)\delta(z-z_s) \quad (7)$$

This equation is a basis that calculates the voltage distribution through the body through point current source. Obtaining voltage distribution form equation (7) is called forward solver [21].

Given a known conductivity in the field and the boundary conditions (which exert excitation current around the field), we wish to determine the electric potential in the field. The ERT sensitivity field can be described as

$$-\nabla\cdot(\sigma\nabla V) = 0 \text{ in } \Pi \quad (8)$$

$$\int_{\Gamma 2}\sigma\frac{\partial V}{\partial n}ds = -I \text{ on source electrode}$$

$$\int_{\Gamma 1}\sigma\frac{\partial V}{\partial n}ds = +I \text{ on sink electrode}$$

$$\frac{\partial V}{\partial n}\Big|_{\Gamma 3} = 0 \text{ others}$$

Where, σ is conductivity; V is potential distribution in the field; Γ1 and Γ2 are the surfaces of the source electrode and sink electrode, respectively; Π is the sensor's internal volume; Γ3 is the insulation surface of the sensor; and n is the outer normal vector on any one point of the boundary [22-23].

II. TOUCH SPECIFICATIONS

To illustrate the specifics of a real touch, we assume the touch pattern is Gaussian curves.

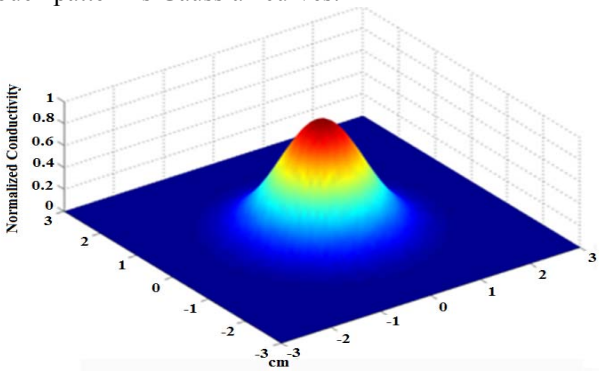

Figure 3. Gaussian-shaped patterns for touch

As seen in Fig. 3, due to the nature of touch with a foreign object, the maximum amount of conductivity is at the tip of the curve. As we get further away from the center, the touch conductivity decreases in a manner that after about 3 to 5 mm radius there is practically no effect on the touch screen.

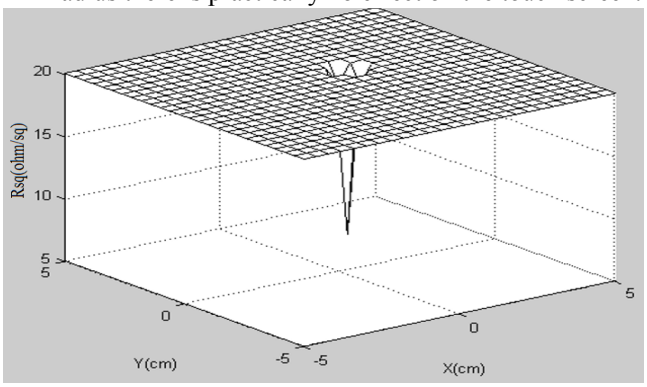

Figure 4. Touch on x=1, y=1 coordinates

Fig. 4 demonstrates the resistance of the touch screen upon touching in x=1 and y=1. It is obvious that resistance in the point of touch equals the minimum value and is in the Gaussian Shape. It is fixed in the rest of the screen. Resistance value at the point of touch equals the resistance of the object being touched.

Touch in different parts of the screen is done experimentally and simulated in MATLAB, then for each point of touch, electrode potential is recorded in two modes.

III. Simulation Results

A. Electric Field and Electric Potential

Fig. 5a shows the pattern of electric field, with a sheet resistance of 20 Ω/sq and boundary conditions mentioned, in PDE Toolbox of MATLAB. This is a very useful tool to solve partial differential equations like equation (7) using conventional finite difference methods.

Fig. 5b shows the lines with equal potential and the value of potential in the screen with no-touch. The highest voltage is in electrode C1 where the current is injected and the lowest voltage, zero, is in electrode C9 that is the base node.

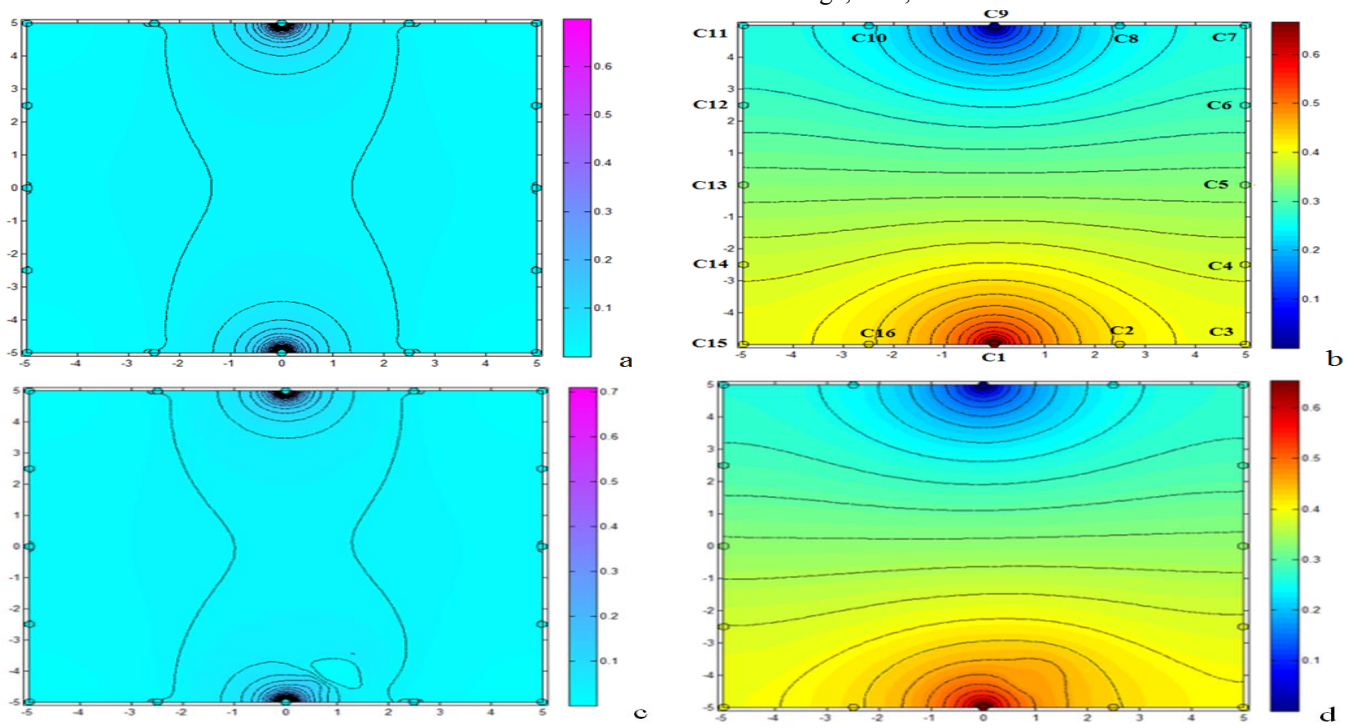

Figure 5. The simulation results for a) electric field lines in a screen with no touch, b) equipotential in a screen with no touch, c) the impact of touch in x=1, y=-4 on the electric field pattern and d) the impact of x=1, y=-4 on electric potential pattern

Fig. 5c shows the electric field pattern change and Fig. 5d shows the potential pattern change at the point of touch with x=1, y=-4 coordinates.

B. Electrode voltage

1) Relative to the Ground

The simulated voltage value of each node to base node in both touch and no-touch modes are shown in Table I. Comparing the electrode voltage for both touch and no-touch modes reveals that the span of voltage from minimum 270.00 mV to maximum 590.00 mV is 320.00 mv. Therefore, a 15-bit ADC is required to achieve such a precision (0.01 mV). Such a system would be susceptible to any external noise since the sensitivity ($S=\Delta V_{min}/V$) in this case will be very small.

Table I. Comparison of the Voltage of the Electrodes

Electrode Voltage(mV)	No Touch	x=1, y=4	x=-3, y=3	x=4, y=2
C2	427.51	413.38	425.85	425.72
C3	401.24	386.70	399.52	399.25
C4	379.91	365.31	378.46	377.84
C5	333.45	318.08	332.11	330.23
C6	286.86	270.42	285.80	288.29
..	..	..	..	..
C16	427.51	414.38	425.42	426.21

2) Differential Voltage of Electrode Pair

In this method, instead of using each electrode's voltage to the node voltage, the voltage difference of the two symmetrical electrodes is considered. As shown in Fig. 5a, lines with similar potential pass through symmetrical electrodes. For example, electrodes C2 to C8 with electrodes C10 to C16, respectively, have the same potential. The differential voltage for two electrodes in the non-touch mode is zero and in the touch mode, depending on the point of touch, can be positive or negative.

The change range is much lower than the previous mode. Table II shows the voltage differential in the previous points. As is specified in the table change range is about ± 8.00 mV. Therefore, an 11-bit ADC is required and the sensitivity value to achieve the same precision value will be quite large. Moreover, due to differential nature of the generated signal, a differential amplifier can be used and consequently most of common mode noises would be removed.

Of course, in a conventional ERT system that deals with heterogeneous material, differential voltage is not very useful.

Table II. Differential Electrode Voltage Achieved from Several Sample Touches

Electrode Voltage(mV)	No Touch	x=1,y=4	x=0,y=3	x=4,y=2
C2-C16	0.0	-1.04	0.0	-0.52
C3-C15	0.0	-1.57	0.0	-0.82
C4-C14	0.0	-1.91	0.0	-1.02
C5-C13	0.0	-3.42	0.0	-2.21
C6-C12	0.0	-5.75	0.0	2.13
C7-C11	0.0	-6.80	0.0	2.82
C8-C10	0.0	-7.06	0.0	1.57

C. Blind spot

The problem with the differential voltage reading method is the blind spots. This means that the imaginary line in the direction of current injection (C1-C9) has a blind spot there and touches on this spot do not create differential changes. If we look at Fig. 6a and Fig. 6b as the point of touches nears the axis of symmetry, the electric field lines and lines with equal potential become more symmetrical. This means zero differential voltage across the pair of electrodes.

To fix this problem in differential electrode pairs, we should introduce a new current injection route and define new pair of differential electrodes that detect blind spots on the symmetry line. One way is to inject a current through C5 and C13 and read the voltage of the other electrodes. This would solve the problem largely. However, the problem of the point of origin remains. Therefore, we put this solution aside and in order to solve the problem electrode C2 is chosen as the point of current injection and the base electrode is chosen to be C8. This will move the current injection line and each touch on the previous symmetry is detectable.

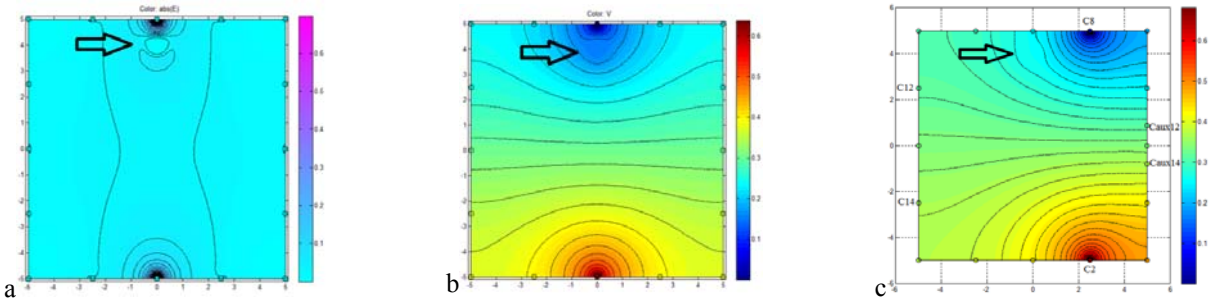

Figure 6. The issue of blind spot in (x = 0, y = 4) 'a' and 'b' field lines and symmetrical potential when the point of touch is on current injection line 'c' fixing the problem by embedding auxiliary electrodes

Now we need to select two pairs of differential electrodes that give zero voltage in no-touch mode. In the existing electrodes such condition does not exist. So we need an auxiliary electrode. Close attention to Fig. 6c reveals that if electrode C14 is considered, its potential pair at x = 5, y = -0.7 will be Caux14 and if we consider C12 as the next electrode, its potential pair at x = 5, y = 0.7 will be called Caux12. According to the new situation in the differential voltages injection and readings, blind spots are covered on the y-axis. Table III shows the aux voltage electrodes for some of the blind spots.

TABLE III. AUXILIARY ELECTRODE VOLTAGE WHEN TOUCHING THE BLIND SPOTS

Electrode Voltage(mV)	C14-Caux14	C12-Caux12	C14	Caux14
No-Touch	0	0	366.6	366.6
x=0,y=4	-1.72	-3.36	361.8	363.5
x=0,y=3	-1.41	-2.07	362.5	363.9
x=0,y=-3	2.03	1.4	367.5	365.5
x=0,y=-2	0.97	1.29	366.3	365.4
x=0,y=-1	0.0	1.04	365.3	365.3
x=0,y=0	-0.50	0.50	364.5	365.0

IV. IMPLEMENTATION

A. Sensor structure

A 10 cm ×10 cm rectangular plate of glass coated with FTO and sheet resistance of 20 Ω /sq is chosen. FTO thickness was considered around 100 nm. 18 circular copper electrodes were placed on the sides of the plates. An independent current source was used to inject 3 mA direct current. The current is injected through C1and C9 (Fig. 7).

B. Stylus

To touch on the touchscreen a stylus with a circular touch point with 1.5 mm radius was used. For the tip of this pen a conductive material such as aluminum was selected so that it could decrease the value of the sheet resistance of the screen upon touching the screen. This change in resistance results in the change of the uniform electric field pattern on the screen and its impact will appear on the side electrodes (Fig. 8).

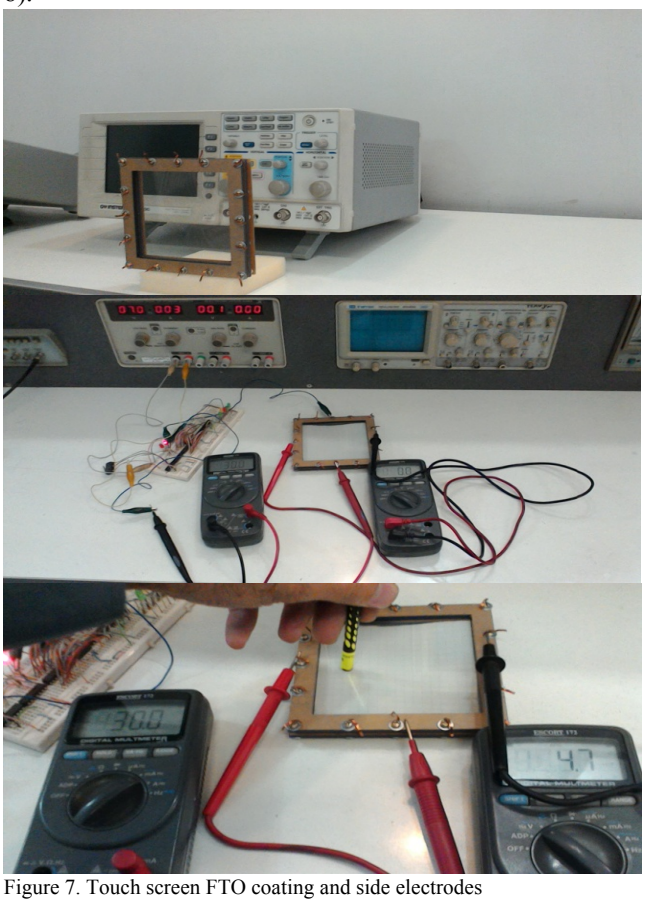

Figure 7. Touch screen FTO coating and side electrodes

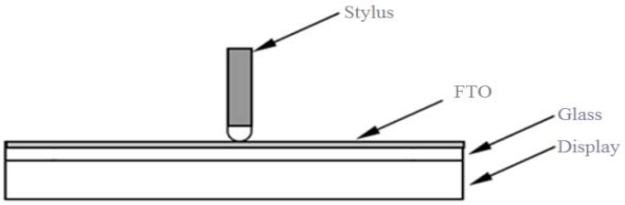

Figure 8. Stylus pen touching the screen

C. Electrodes

For 18 side electrodes silver, aluminum and copper strips were used with circular and rectangular shapes. Since the voltage reading electrodes were connected to a voltmeter with high impedance therefore, the material had no significant impact on the amount of output voltage. Also rectangular electrodes caused non-uniformity in current density. Thus, as shown in Fig. 9 circular electrodes were selected.

The material difference between FTO and the electrodes in the point of touch resulted in thermocouple effect. This phenomenon when receiving differential electrode voltage is neutral and does not affect output data.

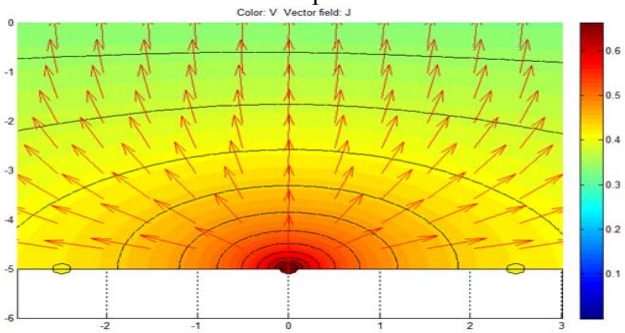

Figure 9. Uniform current density with circular electrodes

V. Experimental Results

The electrodes differential voltage C2-C8 to C10-C16, as well as auxiliary electrodes in a state of non-touch and touch are collected. An example of this voltage for all the touch points is presented in Table IV.

TABLE IV. EXPERIMENTAL ELECTRODE VOLTAGE FIGURES FOR NO TOUCH MODE AND SOME SAMPLE TOUCHES

Electrode Voltage (mV)	No Touch	x=1,y=4	x=-3,y=3	x=0,y=0	x=0,y=-3
C2-C16	0.01	-1.01	0.41	0.0	-0.01
C3-C15	0.01	-1.50	0.59	0.0	-0.01
C4-C14	-0.01	-1.89	0.80	-0.01	-0.01
C5-C13	0.0	-3.39	1.61	0.0	0.01
C6-C12	0.01	-5.71	2.10	0.0	-0.01
C7-C11	0.01	-6.80	-0.60	-0.01	-0.01
C8-C10	-0.01	-7.01	-2.32	-0.01	0.0
C14-Caux14	0.0	-2.19	-0.50	-0.5	-1.38
C12-Caux12	0.0	-4.28	-1.21	0.50	-2.03

A. Comparing Experimental Results and the Simulation

Touch points were selected with a distance of 0.5 cm from each other in two directions of x, y (to cover the whole page) and in every touch the voltage of the electrode pairs (7 main pairs and 2 auxiliary pairs) were measured.

The comparison of the experimental and the simulation values of the electrodes for these 361 touches points for every sample electrode pair from among 9 pairs shown in Fig. 10 reveal that the maximum relative error margin for these two is 1.4%. The highest errors occurred in points closer to the electrodes. This amount of error shows the acceptable precision of the simulation model.

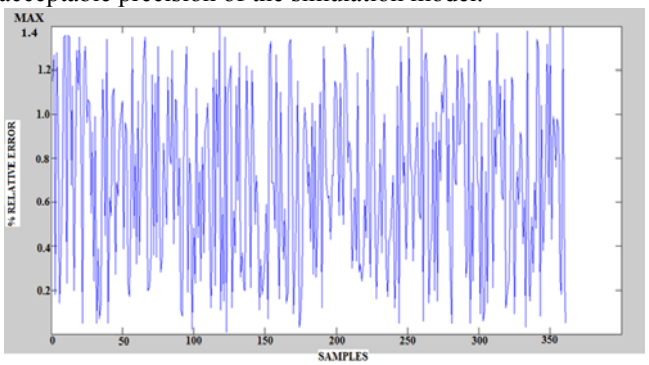

Figure 10. The difference of the measured value and the simulated data in a sample electrode pair

B. The Effect of Stylus Radius on Electrode Voltages

The effect of the diameter of the touch on measuring electrode voltage was investigated. As Fig. 11 shows a route was set for stylus touch on the screen so that it covered most parts of the screen. Voltage curve of all pairs of electrodes when stylus moved from point A (-4.5, -4.5) to point B (0, 0) were sampled. To do so three types of styluses with three radiuses of R1 = 1 mm, R2 = 1.5 mm, R3 = 3 mm were utilized. The maximum range of the electrode voltage changes in the radius R1, R2, R3, were 12 mV, 16 mV, 24 mV, respectively. In Fig. 12 voltages of a pair of electrodes are shown.

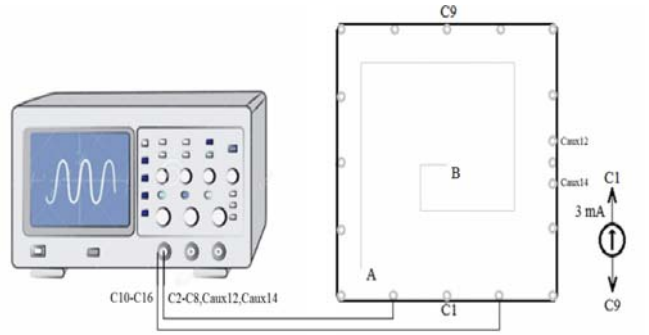

Figure 11. Measuring stylus radius effects on electrode voltages

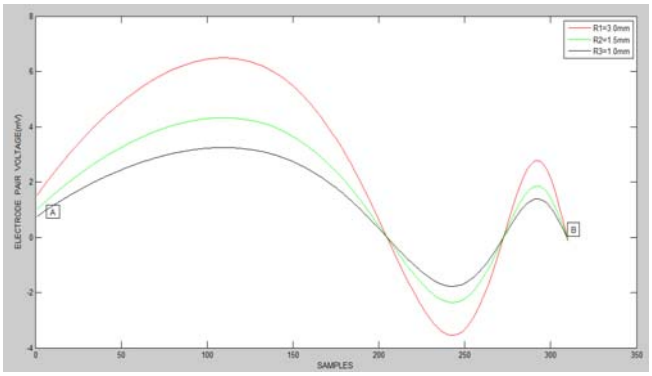

Figure 12. Electrode voltage curve in three different stylus stages

VI. Conclusion

A square glass plate with 10 cm ×10 cm dimension, coated with FTO and sheet resistance of 20 Ω /sq was chosen. 16 main electrodes and 2 auxiliary electrodes were

placed on sides of screen. A 3 mA direct current was injected through electrodes by a current source in the screen. The differential voltage of electrodes was read. 9 voltage readings were recorded for every touch. A stylus pen with 1.5 mm radius and a conductive tip was used to touch the screen. When there were no touches on the screen, all the voltages equaled zero. When the stylus made the touch, a voltage relative to the coordinates of the touch in electrodes is read. The voltage change range was ±8.00 mV. The maximum error margin between the experimental results and the simulations was 1.4%. This amount of error shows the acceptable precision of the simulation model. The change in touch area of the stylus in three different radiuses of 1, 1.5 and 3 mm showed that the electrode voltage change range was 12 mV, 16 mV and 24 mV respectively.

This screen with a maximum optical transmittance and without any patterning was able to convert the touch point coordinates into electrode voltages.

The advantages of this sensor are as follows:

1) Using uniform coating techniques instead of patterned ones which are costly and complicated.

2) Receiving the differential voltage with a higher signal to noise ratio relative to the single mode.

3) Using a cheap TCO such as FTO instead of ITO.

4) Embedding side electrodes to maximize transmittance.

REFERENCES

[1] M. R. Bhalla, A. V. Bhalla, "Comparative study of various touchscreen technologies," International Journal of Computer Applications, vol. 6, pp. 12-18, 2010. doi:10.5120/1097-1433

[2] S. M. Hong, Y. F. Tan, H. S. Yeo, B. G. Lee, "1-inch UniTouch System using Kinect," In Signal Processing Image Processing & Pattern Recognition (ICSIPR), pp. 351-355. Feb. 2013. doi: 10.1109/ICSIPR.2013.6497994

[3] J. Lee, M. T. Cole, J. C. S. Lai, A. Nathan, "An analysis of electrode patterns in capacitive touch screen panels," Journal of Display Technology, vol. 10, pp. 362-366, 2014. doi:10.1109/JDT.2014.2303980

[4] K. Lim, K. S. Jung, C. S. Jang, J. S. Baek, I. B. Kang, "A fast and energy efficient single-chip touch controller for tablet touch applications," Journal of Display Technology, vol. 9, pp. 520-526, 2013. doi:10.1109/JDT.2013.2243900

[5] B. Y. Won, J. Ki Ahn, H. Gyu Park "New Surface Capacitive Touchscreen Technology To Detect DNA," ACS Sensors, vol. 1, pp. 560–565, 2016. doi: 10.1021/acssensors.6b00040

[6] M. G. Mohamed, T.-W. Cho, and H. Kim, "Efficient multitouch detection algorithm for large touch screen panels," IEIE Transactions on Smart Processing and Computing, vol. 3, no. 4, pp. 246–250, 2014. doi:10.5573/IEIESPC.2014.3.4.246

[7] A. Stadler, "Transparent conducting oxides—An up-to-date overview," Materials, vol. 5, pp. 661-683, 2012. doi:10.3390/ma5040661

[8] J. Lee, S. Lee, G. Li, M. A. Petruska, D. C. Paine, S. Sun, "A facile solution-phase approach to transparent and conducting ITO nanocrystal assemblies," Journal of the American Chemical Society, vol. 134, pp. 13410-13414, 2012. doi:10.1021/ja3044807

[9] M. Kang, K. InKoo, C. Minwoo, W. K. Sok, "Optical Properties of Sputtered Indium-tin-oxide Thin Films," Journal of the Korean Physical Society, vol. 59, pp. 3280-3283, 2011. doi:10.3938/jkps.59.3280

[10] A. Kumar, C. Zhou, "The race to replace tin-doped indium oxide: which material will win?," ACS nano, vol. 4, pp. 11-14, 2010. doi:10.1021/nn901903b

[11] M. A. Aouaj, R. Diaz, A. Belayachi, F. Rueda, M. Abd-Lefdil, "Comparative study of ITO and FTO thin films grown by spray pyrolysis," Materials Research Bulletin, vol. 44, pp. 1458-1461, 2009. doi:10.1016/j.materresbull.2009.02.019

[12] V. Bilgin, I. Akyuz, E. Ketenci, S. Kose, F. Atay, "Electrical, structural and surface properties of fluorine doped tin oxide films," Applied Surface Science, vol. 256, pp. 6586-6591, 2010. doi:10.1016/j.apsusc.2010.04.052

[13] W. Samad, M. S. Muhamad, S. Ashkan, A. Y. Mohd, "Structural, Optical and Electrical Properties of Fluorine Doped Tin Oxide Thin Films Deposited Using Inkjet Printing Technique," Sains Malaysiana, vol. 40, pp. 251–257, 2011.

[14] B. P. Singh, R. Kumar, A. Kumar, J. Gaur, S. P. Singh, R. C. Tyagi, "Effect of annealing on properties of transparent conducting tin oxide films deposited by thermal evaporation," Indian Journal of Pure and Applied Physics, vol. 51, pp. 558-562, 2013.

[15] Z. Y. Banyamin, P. J. Kelly, G. West, J. Boardman, "Electrical and optical properties of fluorine doped tin oxide thin films prepared by magnetron sputtering," Coatings, vol. 4, pp. 732-746, 2014. doi:10.3390/coatings4040732

[16] D. W. Sheel, J. M. Gaskell, "Deposition of fluorine doped indium oxide by atmospheric pressure chemical vapour deposition" Thin Solid Films, vol. 520, pp. 1242-1245, 2011. doi:10.1016/j.tsf.2011.04.206

[17] P.V. Bhuvaneswari, P. Velusamy, R.R. Babu, S.M. Babu, K. Ramamurthi, M. Arivanandhan, "Effect of fluorine doping on the structural, optical and electrical properties of spray deposited cadmium stannate thin films," Mater. Sci. Semicond. Proc. vol. 16, pp. 1964–1970, 2013. doi:10.1016/j.mssp.2013.07.025

[18] M. Sharifi, B. Young, "Electrical resistance tomography (ERT) applications to chemical engineering," Chemical Engineering Research and Design, vol. 91, pp. 1625-1645, 2013. doi:10.1016/j.cherd.2013.05.026

[19] L. Orlando, "GPR to constrain ERT data inversion in cavity searching: Theoretical and practical applications in archeology," Journal of Applied Geophysics, vol. 89, pp. 35-47, 2013. doi:10.1016/j.jappgeo.2012.11.006

[20] J. Frounchi, K. Samadzamini, H. Taghipour, "Design and Implementation of an Electrostatic Analyzer on a FPGA for Electrical Resistance Tomography Systems," Proc. 13th Joint International and National CSI Computer (Kish Island), Kish, Iran, 2008.

[21] T. Gunther, C. Rucker, K. Spitzer, "Three-dimensional modeling and inversion of DC resistivity data incorporating-II inversion," Geophysical Journal International, vol. 166, pp. 506-517, July 2006. doi:10.1111/j.1365-246X.2006.03010.x

[22] P. Wang, B. Guo, "Multiple Index Optimization Method Based on Orthogonal Design and Fuzzy Analysis for ERT Sensor Design," International Journal of Engineering & Industries, vol. 3, 2012. doi:10.4156/ijei.vol3.issue3.5

[23] F. Dong, C. Tan, J. Liu, Y. Xu, H. Wang, "Development of single drive electrode electrical resistance tomography system," IEEE transactions on instrumentation and measurement, vol. 55, pp. 1208-1214, 2006. doi:10.1109/TIM.2006.877751